The drag of a compressible turbulent boundary layer on a smooth flat plate with and without heat transfer

By D. B. SPALDING and S. W. CHI
Mechanical Engineering Department,
Imperial College of Science and Technology, London, S.W. 7

(Received 10 May 1963)

The theoretical treatments given by earlier authors are classified, reviewed and where necessary extended; then the predictions of twenty of these theories are evaluated and compared with all available experimental data, the root-mean-square error being computed for each theory. The theory of van Driest–II gives the lowest root-mean-square error (11·0 %).

A new calculation procedure is developed from the postulate that a unique relation exists between $c_f F_c$ and RF_R where c_f is the drag coefficient, R is the Reynolds number, and F_c and F_R are functions of Mach number and temperature ratio alone. The experimental data are found to be too scanty for both F_c and F_R to be deduced empirically, so F_c is calculated by means of mixing-length theory and F_R is found semi-empirically. Tables and charts of values of F_c and F_R are presented for a wide range of M_G and T_S/T_G. When compared with all experimental data, the predictions of the new procedure give a root-mean-square error of 9·9 %.

1. Introduction

In many circumstances of interest to aeronautical engineers, it is necessary to predict the frictional drag at a surface along which a gas is flowing at high speed and through which heat is being transferred. This is not only important in the prediction of the frictional drag itself but also in the prediction of the heat transfer, for example by means of a 'modified Reynolds analogy'. This knowledge is required in connexion with many processes, for example, in the cooling of combustion-chamber walls, gas-turbine blades, hypersonic ram-jet intakes, rocket-motor nozzles and high-speed aircraft skins.

Often the velocity of the mainstream fluid is not uniform. In a rocket-nozzle it increases with distance downstream, whilst in a ram-jet intake it decreases; the main-stream pressure is accordingly non-uniform. Despite these facts, it is necessary to restrict attention in the present paper mainly to the case in which the pressure gradient is zero; that is, to that of the boundary layer on a flat plate. The reason is that this is the simplest case, which must be understood first.

There have been numerous investigations of the problem, both theoretical and experimental; these will be described in some detail in the following §§2, 3. Nevertheless, as will appear below, present knowledge of the subject is defective in two respects. First, there is considerable uncertainty as to which of various theories gives the best prediction; for each theory contains fairly drastic simplifications, and has usually been compared with only a small selection of the available experimental data. Secondly, some of the methods of prediction (including unfortunately those which give the most accurate predictions) are difficult to use; the prospective user of the method has to carry out extensive numerical work, because the necessary auxiliary functions have not been computed and tabulated once for all.

It is intended below to pay particular attention to remedying the above defects. As far as possible, uncertainty will be eliminated by comparing the existing theories with all published experimental data and by developing a new calculation procedure based upon accumulated theoretical and experimental knowledge of the compressible turbulent boundary layer; and graphs and tables will be presented which permit friction to be calculated for a wide range of conditions as a result of merely a few minutes' work.

The tables cover Mach numbers (M_G) between 0 and 15, and ratios of wall temperature to main-stream temperature (T_S/T_G) between 0·05 and 30.

Sections 2 and 3 below are mainly devoted to a review of earlier work. These lead to a development of the present method which is presented in §4. Readers solely concerned with the use of the method should turn to §4.6 which contains a summary of the prediction procedures which are recommended for use.

Notation

a, b	see equations (13) and (14)
c_f	local frictional drag coefficients based upon main-stream fluid properties, equation (17)
$\bar{c}_f$	overall frictional drag coefficient based upon main-stream fluid properties, equation (26)
E	a constant, equation (2)
F_c	function multiplying c_f in universal drag law, equations (11) and (19)
$F_{\bar{c}}$	function multiplying $\bar{c}_f$ in universal drag law, equation (11)
$F_{R\delta}$	function multiplying R_δ in universal drag law, equations (12) and (20)
F_{Rx}	function multiplying R_x in universal drag law, equations (12) and (25)
h	specific enthalpy, equation (32), (B.Th.U./lb.)
h^0	stagnation enthalpy, equation (32), (B.Th.U./lb.)
K	a constant ($\approx 0{\cdot}4$), equation (2)
M_G	Mach number of main stream, equation (13)
n, p, q	exponents, equations (44) and (51)
P	Prandtl number, equation (36)
r	recovery factor, equation (35)
R_δ	Reynolds number based upon momentum thickness and main-stream fluid properties, equation (3)
R_x	Reynolds number based upon x and main-stream fluid properties, equation (21)
T	temperature, equation (13), (°R)
u	velocity in x-direction, equation (1), (ft./h)
x	distance measured along main-stream direction from effective start of turbulent boundary layer, implied in the definition of R_x, (ft.)

u^+	non-dimensional value of u, equation (2)
y	distance from wall, equation (1), (ft.)
y^+	non-dimensional value of y, equation (2)
z	a different non-dimensional value of u, equation (2)
δ_2	momentum thickness, equation (3), (ft.)
γ	specific heat ratio, equation (13)
ϕ	function appearing in equations (2), (5), etc.
$\left.\begin{array}{l}\psi_\delta\\ \psi_x\\ \overline{\psi}\end{array}\right\}$	functions appearing in the generalized drag laws, equations (18), (24) and (27)
ρ	density, equation (1), (lb./ft.^{3})
μ	viscosity, equation (3), (lb./ft.h)
τ	shear stress in boundary layer, equation (1), (lb./ft.h^2)

Subscripts

av	average conditions in laminar sublayer
G	main-stream fluid state, equation (2)
i	uniform property flow, equation (43)
N	state near the wall, equation (43)
S	state at the wall, equation (2)
1	outer edge of laminar sublayer, table 1

2. Survey of previous theoretical work

2.1. *General characteristics of analyses*

There are a number of theories for the prediction of the frictional-drag coefficient in the compressible turbulent boundary layer on a smooth flat plate (see the references marked with an asterisk in the list at the end of the paper). According to the nature of the principal assumptions used by various authors, the theories can be grouped into five types, namely, (i) theories based upon the Prandtl differential equation, (ii) theories based upon the von Kármán differential equation, (iii) theories based upon other differential equations, (iv) theories based upon a fixed velocity profile, and (v) theories based upon the incompressible formulae with fluid properties inserted at a 'reference' state. The main features of the analyses for each of those groups will be summarized in the following five sections (§§ 2.2–2.6), and the characteristics of individual theories belonging to these groups will be indicated in tables 1–5. Table 6 includes miscellaneous analyses which do not belong to any of the five groups mentioned above.

2.2. *Theories based upon the Prandtl differential equation*

By 'the Prandtl differential equation' we mean that postulated by Prandtl (see Schlichting 1960, p. 477) relating the shear stress in the turbulent part of the boundary layer to the velocity gradient and other properties, namely

$$\tau = \rho K y^2 \left(\frac{du}{dy}\right). \tag{1}$$

Author and year	Hypothesis for E	Nature of ϕ	Method of evaluating R_δ integral
Smith & Harrop (1946)	$E = 11{\cdot}24$		Approximate analytical (A)*
van Driest–I (1951)	$E = 13{\cdot}1$ (for ψ_x)†		Approximate analytical (B)*
Kalikman (1956)	$2y_1 u_{av}\rho_{av}/\mu_{av} = (11{\cdot}5)^2$ $y_1^+ = u_G^+(z_1 + \frac{1}{2}bPz_1^2 + \frac{1}{3}bPz_1^3)$	$\phi = (\rho/\rho_S)^{\frac{1}{2}} = (1 + bz - a^2z^2)^{-\frac{1}{2}}$	Exact numerical
Dorrance (1960)	$E = 13{\cdot}1$ (for ψ_x)		Exact numerical (approximate integration used later to yield $c_f(R_x)$
Kutateladze & Leont'ev (1961)	$y_1^+ = 11{\cdot}6(T_G/T_S)^{\omega+\frac{1}{2}}$ $z_1 = 11{\cdot}6 \times (\frac{1}{2}$ drag coefficient in uniform-property flow at same $R_\delta)^{\frac{1}{2}}$	$\phi = (\rho/\rho_S)^{\frac{1}{2}} = [1 + (b - 0{\cdot}1a^2)z - 0{\cdot}9a^2z^2]^{-\frac{1}{2}}$	Approximate analytical (B)

* These methods of evaluating R_δ integral are summarized in the Appendix.
† 'For ψ_x' means that the value of E specified here is for the c_f *vs.* R_x expression.

TABLE 1. Theories based upon Prandtl differential equation

Author and year	Hypothesis for E	Nature of ϕ	Method of evaluating R_δ integral
Frankl & Voishel (1937)	$u_1^+ = 11{\cdot}5$ $(du^+/dy^+)_1 = 0{\cdot}289$	$\phi = (\rho/\rho_S)^{\frac{1}{2}} = (1 + bz - a^2z^2)^{-\frac{1}{2}}$	Approximate analytical—by expanding integrand in series of b and a^2, and neglecting higher terms
Wilson (1950)	$u_1^+ = 11{\cdot}6$ $(du^+/dy^+)_1 = 0{\cdot}218$	$\phi = (\rho/\rho_S)^{\frac{1}{2}} = (1 - a^2z^2)^{-\frac{1}{2}}$ (adiabatic only)	Approximate analytical (B)
Rubesin, Maydew & Varga (1951)	$u_1^+ = 11{\cdot}5$ $(du^+/dy^+)_1 = 0{\cdot}218$	$\phi = (\rho/\rho_S)^{\frac{1}{2}} = (1 + bz - a^2z^2)^{-\frac{1}{2}}$	Exact numerical
van Driest–II (1955)	$E = 13{\cdot}1$ (for ψ_x)		Approximate analytical (B)
Deissler & Loeffler (1959)	$y_1^+ = 26$ For $y^+ \leqslant 26$, $\tau_S = (\mu + 0{\cdot}01188\rho uy)\dfrac{du}{dy}$ $q_S = (k + 0{\cdot}01188\rho uy)\dfrac{dT}{dy}$	$\phi = (\rho/\rho_S)^{\frac{1}{2}} = \left[\dfrac{T_1}{T_S} - \dfrac{q_S}{c_p T_S \sqrt{(\rho_S \tau_S)}}(u^+ - u_1^+) - \dfrac{\tau_S}{2c_p T_S \rho_S}(u^{+2} - u_1^{+2})\right]^{-\frac{1}{2}}$	Exact numerical

TABLE 2. Theories based upon von Kármán differential equation

Author and year	Nature of differential equation	Method of evaluating R_δ integral
Clemmow-I (1950)	$\tau_S = \rho K^2 y^2 \left(\frac{du}{dy}\right)^2 + uK^2 y^2 \frac{du}{dy}$	Approximate analytical (B)
Clemmow-II (1950)	$\tau_S = K^2 \frac{(du/dy)^3}{(d^2u/dy^2)^2}\left(\rho \frac{du}{dy} + u \frac{d\rho}{dy}\right)$	
Ferrari (1950)	$\sqrt{\frac{\tau_S}{\rho_S}} = \frac{\rho Ky(du/dy)}{\rho_S\left\{1+\text{const.}\times z\left[1+\frac{2}{(\gamma-1)M_G^2}\right]^{-\frac{1}{2}}\right\}}$ The value of constant is unknown	Approximate numerical
Li & Nagamatsu (1951)	$\tau_S = \rho K^2 y^2 (du/dy)^2 + f(M_G) uK^2 y^2 \frac{d\rho}{dy}\frac{du}{dy}$ The function of M_G, $f(M_G)$ is unknown	Approximate analytical (B)
Kosterin & Koshmarov (1960)	$\tau_S = \rho K^2 y^2 (du/dy)^2 + \int K^2 yu \frac{d\rho}{dy}\frac{du}{dy}\,dy$	Exact numerical

TABLE 3. Theories based upon other differential equations

Author and year	Assumed velocity profile	Expression of ρ/ρ_S	Method of evaluating R_δ integral
Cope–I (1943)	$u^+ = 8{\cdot}7y^{+\frac{1}{7}}$	$\rho/\rho_S = (1-a^2z^2)^{-1}$ (adiabatic only)	Exact numerical
Cope–II (1943)	$y^+ = E^{-1}\exp(Ku^+)$		Approximate analytical (B)
Monaghan (1950)	$y^+ = E^{-1}\exp(Ku^+)$	$\rho/\rho_S = (1+bz-a^2z^2)^{-1}$	Approximate analytical (B)

TABLE 4. Theories based upon fixed velocity profile

Author and year	Expression of T_R/T_G
von Kármán (1935)	$T_R/T_G = 1+\frac{1}{2}(\gamma-1)M_G^2$ (adiabatic only)
Tucker (1951)	$T_R/T_G = 1+\frac{1}{4}(\gamma-1)M_G^2$ (adiabatic only)
Young & Janssen (1952)	For $M_G < 5{\cdot}6$: $T_R/T_G = 0{\cdot}42+0{\cdot}58(T_S/T_G)+0{\cdot}035\,M_G^2$ For $M_G > 5{\cdot}6$: $T_R/T_G = 0{\cdot}42+0{\cdot}58(T_S/T_G)+0{\cdot}023\,M_G^2$
Sommer & Short (1955)	$T_R/T_G = 0{\cdot}55+0{\cdot}45(T_S/T_G)+0{\cdot}035M_G^2$
Eckert (1955)	$T_R/T_G = 0{\cdot}5+0{\cdot}5(T_S/T_G)+0{\cdot}11P^{\frac{1}{3}}(\gamma-1)M_G^2$ or $h_R/h_G = 0{\cdot}28+0{\cdot}5(h_S/h_G)+0{\cdot}22(h_{ad,S}/h_G)$

TABLE 5. Theories based upon incompressible formulae (ψ_x) with reference properties

With the assumption $\tau = \tau_S$, the velocity distribution in the turbulent boundary layer is derived,

$$y^+ = E^{-1}\exp\left(Ku_G^+\int_0^z \phi\,dz\right), \tag{2}$$

where $y^+ \equiv y(\tau_S\rho_S)^{\frac{1}{2}}/\mu_S$, $u^+ \equiv u/(\tau_S/\rho_S)^{\frac{1}{2}}$, $z \equiv u/u_G$, $\phi \equiv (\rho/\rho_S)^{\frac{1}{2}}$, K = a mixing length constant, E = an integrating constant, and subscript G refers to the main stream, i.e. the outer 'edge' of the boundary layer, subscript S refers to the fluid conditions immediately adjacent to the wall, i.e. to the inner 'edge' of the boundary layer.*

Equation (2) leads to the integral for R_δ:

$$R_\delta = \frac{\mu_S}{\mu_G}\frac{K}{E}(u_G^+)^2\int_0^1 \phi^3 z(1-z)\exp\left(Ku_G^+\int_0^z \phi\,dz\right)dz, \tag{3}$$

where $$R_\delta \equiv \frac{\rho_G u_G \delta_2}{\mu_G}, \quad \delta_2 \equiv \int_0^{y_G}\frac{\rho}{\rho_G}\frac{u}{u_G}\left(1-\frac{u}{u_G}\right)dy.$$

The above features are common to all analyses of this group. The differences between them are in either: (i) an hypothesis for E (or other method of determining the integration constant), (ii) the nature of the ϕ function, or (iii) the method of evaluating the R_δ integral. Accordingly, the individual members of the group are distinguished by the nature of these three items in table 1.

2.3. *Theories based upon the von Kármán differential equation*

The differential equation postulated by von Kármán (see Schlichting 1960, p. 485) as the connexion between τ, du/dy and other quantities is

$$\tau = \rho K^2 (du/dy)^4/(d^2u/dy^2)^2. \tag{4}$$

The assumption $\tau = \tau_S$ leads to the velocity distribution

$$y^+ = (K/E)\int_0^{u^+}\exp\left(Ku_G^+\int_0^z \phi\,dz\right)du^+. \tag{5}$$

This leads further to the R_δ integral

$$R_\delta = \frac{\mu_S}{\mu_G}\frac{K}{E}u_G^{+2}\int_0^1 \phi^2 z(1-z)\exp\left(Ku_G^+\int_0^z \phi\,dz\right)dz. \tag{6}$$

Equations (4)–(6) are common to all the methods of this group; individual methods are classified in table 2 by reference to either (i) their hypotheses for E, (ii) the nature of the ϕ function, or (iii) the method of evaluating the R_δ integral.

2.4. *Theories based upon other differential equations*

Analyses of this group start from various differential equations but the assumption of $\tau = \tau_S$ is also made as in the above two groups (§§ 2.2, 2.3). Generally speaking, all proposed differential equations lead to equations for the velocity distribution which are identical in form with (2) or (5). However, the nature of ϕ in this expression differs from that in §§ 2.2 and 2.3, that is, ϕ here is no longer

* A mnemonic: $G \equiv$ gas stream; $S \equiv$ surface.

equal to $(\rho/\rho_S)^{\frac{1}{2}}$. The Reynolds-number integral for the analyses of the group is either

$$R_\delta = \frac{\mu_S}{\mu_G}\frac{K}{E}u_G^{+2}\int_0^1 \phi\frac{\rho}{\rho_S}z(1-z)\exp\left(Ku_G^+\int_0^z \phi\,dz\right)dz, \tag{7}$$

or

$$R_\delta = \frac{\mu_S}{\mu_G}\frac{K}{E}u_G^{+2}\int_0^1 \frac{\rho}{\rho_S}z(1-z)\exp\left(Ku_G^+\int_0^z \phi\,dz\right)dz, \tag{8}$$

depending on whether the velocity distribution of (2) or that of (5) is appropriate. Methods of this group are distinguished in table 3 by reference to either (i) the nature of the differential equation, or (ii) the method of evaluating the R_δ integral.

2.5. *Theories based upon a fixed velocity profile*

In this group, it is assumed that the velocity profile is independent of compressibility, for example,

$$y^+ = E^{-1}\exp(Ku^+), \tag{9}$$

for which the R_δ integral becomes

$$R_\delta = \frac{\mu_S}{\mu_G}\frac{K}{E}u_G^{+2}\int_0^1 \frac{\rho}{\rho_S}z(1-z)\exp(Ku_G^+)\,dz. \tag{10}$$

Methods of this group are distinguished in table 4 by reference to (i) the assumed fixed velocity profile, (ii) the expression for ρ/ρ_S, and (iii) the method of evaluating the R_δ integral.

2.6. *Theories based upon incompressible formulae with reference properties*

Methods of this group imply the existence of a universal relationship between frictional-drag coefficient and Reynolds number, if properties are evaluated at a reference temperature (or reference enthalpy). They are distinguished in table 5 by reference to (i) the method by which the reference temperature was determined, and (ii) the expression for T_R/T_G or (h_R/h_G).

2.7. *Miscellaneous other methods*

Methods which do not belong to those groups discussed in §§ 2.2–2.6 include the use of various transformations and the direct use of empirical data. We have placed in this category the theories of Lin & Shen (1951), Shen (1951), Donaldson (1952), Spence (1959), Winkler (1961), Burgraff (1962) and Coles (1962).

The validity of the assumptions and simplifications involved in various theories can only be verified by comparison with experiment. This will be done systematically in the next section.

3. Comparison between the theoretically and experimentally obtained data

3.1. *Purpose of comparison*

As pointed out above, all theoretical treatments discussed in § 2 have been based upon assumptions and simplifications. Further, their predictions differ significantly, as has been shown, for example, by Chapman & Kester (1953) for the adiabatic-wall case. It is therefore necessary to establish the relative validity of all theories by comparing them with experimental data. Other authors, for example, Rubesin, Maydew & Varga (1951), Sommer & Short (1955), Monaghan (1950), Matting, Chapman, Nyholm & Thomas (1961), Winkler (1961) and Peterson (1963) have compared some theories with experiments; but they either used relatively few sets of experimental data or used a qualitative method of comparison in the form of numerous figures, so their conclusions are still rather indecisive. We shall compare the various theories with all published experimental data of c_f and $\bar{c}_f$ versus R_δ and R_x at various M_G and T_S/T_G, and shall evaluate for each theory a quantitative measure of its agreement with experiment. After that, we shall be able to see which of the available theories is best, and so learn which assumptions for the compressible turbulent boundary layer are most plausible. This examination forms the starting point for the development of an improved calculation procedure, which is also presented below.

3.2. *Experimental data*

If experimental data were accurate, a few sets of data at desired conditions (Mach number and heat-transfer rates) would suffice to test the validity of the various theories. Such data are, however, not available. For this reason, the greatest possible number of experimental data have been collected (see references marked with a double dagger) and tabulated.* They include measurements on a flat plate and on a cylinder with axis parallel to the stream direction and radius large in comparison with the boundary-layer thickness. Figures 1–3 show the collected data in the form of c_f *vs* R_δ, c_f *vs* R_x and $\bar{c}_f$ *vs* R_x, and figure 4 shows the conditions (i.e. values of M_G and T_S/T_G) which have been explored experimentally. Although it must be expected that the data are not all equally reliable, we have made no attempt to estimate their accuracy or to introduce any corresponding weighting factors.

3.3. *Theoretical data*

Theoretical friction-coefficient data corresponding to the experimental Reynolds number (R_δ or R_x), Mach number (M_G) and temperature ratio (T_S/T_G) have been obtained by the various methods discussed in § 2; however, some authors have not worked out all the relations which are required if their theories are to be compared with all the collected experimental data. Extensions can, however, be made to those theories without conflicting with the authors' original argument. The methods used by us in making the extensions are summarized below.

Conversion of R_x to R_δ and vice versa. The results of some analyses, viz. Clemmow (1950), Cope (1943), Monaghan (1950), Smith & Harrop (1946), Van Driest (1950, 1955), Wilson (1950) and the theories of table 5, imply that a unique relation exists between $c_f F_c$ and RF_R where F_c and F_R are functions of Mach number and temperature ratio alone. As will be shown in § 4, the relations between F_c, $F_{\bar{c}}$, $F_{R\delta}$ and F_{Rx} are such that

$$F_c = F_{\bar{c}}, \tag{11}$$

$$F_{Rx} = F_{R\delta}/F_c, \tag{12}$$

where F_c and $F_{\bar{c}}$ are the functions of M_G and T_S/T_G multiplying c_f and $\bar{c}_f$ respectively, and $F_{R\delta}$ and F_{Rx} are the functions of M_G and T_S/T_G multiplying R_δ and R_x,

* The table is not printed here. Copies may be obtained by interested readers on application to the authors.

respectively. Hence equations (11) and (12) enable the determination of the c_f *vs* R_x relation of one of these theories from the corresponding $\bar{c}_f$ *vs* R_x or c_f *vs* R_δ relations, and vice versa.

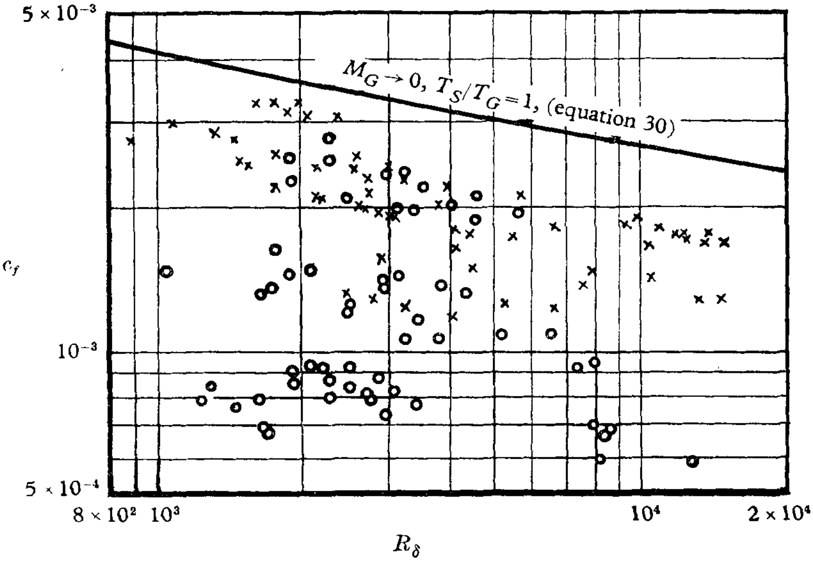

FIGURE 1. Collected experimental data of c_f *vs* R_δ in compressible turbulent boundary layer. ×, adiabatic; ○, with heat transfer.

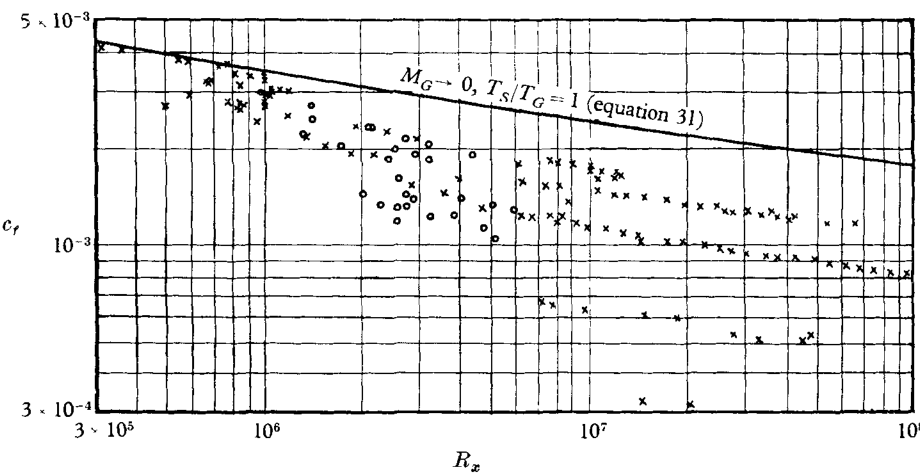

FIGURE 2. Collected experimental data of c_f *vs* R_x in compressible turbulent boundary layer. ×, adiabatic; ○, with heat transfer.

Extension of theories derived for the adiabatic wall to the case of heat transfer. When only the adiabatic-wall case is considered and the Reynolds analogy between momentum and energy transfer is assumed, as in the theories of Cope (1943), Donaldson (1952), Wilson (1950), etc., the temperature-distribution equation is

$$T/T_S = 1 - a^2 z^2, \tag{13}$$

where $$a^2 \equiv [\tfrac{1}{2}(\gamma-1)\,M_G^2]/(1+\tfrac{1}{2}(\gamma-1)M_G^2),$$

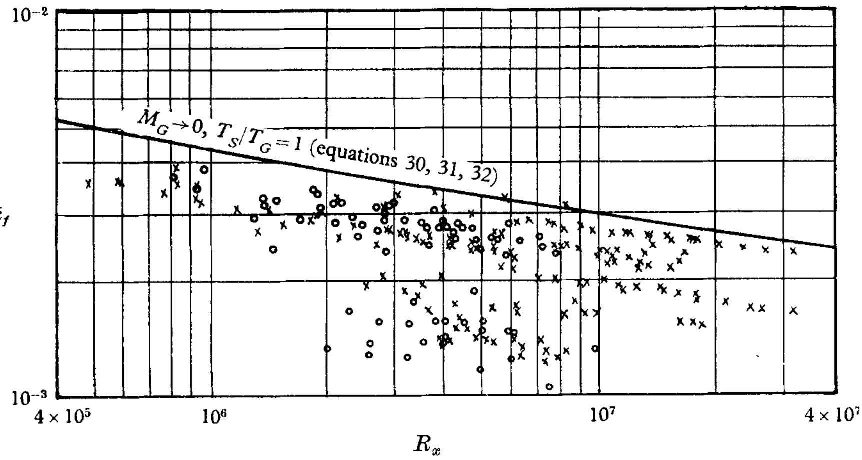

FIGURE 3. Collected experimental data of $\bar{c}_f$ *vs* R_x in compressible turbulent boundary layer. ×, adiabatic; ○, with heat transfer.

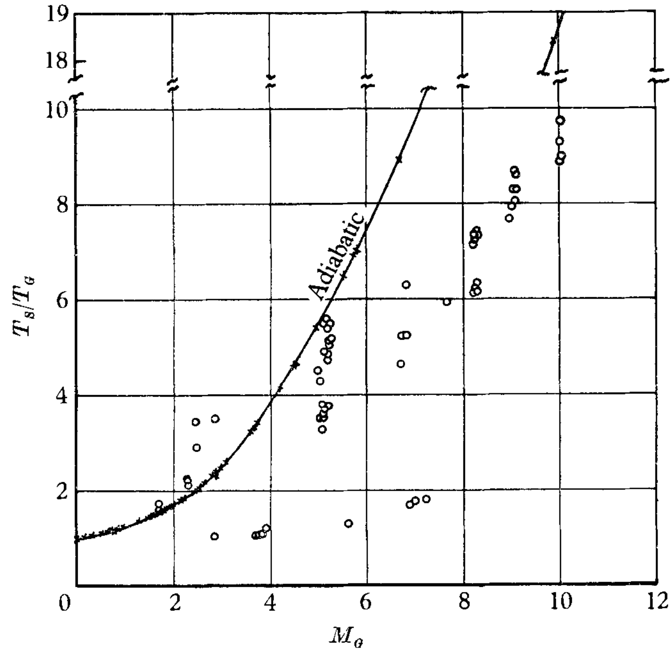

FIGURE 4. Area of conditions explored experimentally.

$z \equiv u/u_G$, $T \equiv$ absolute temperature (°R), and suffixes G and S refer to free stream and surface, respectively.

We have extended equation (13) to include the effect of heat transfer as follows:

$$T/T_S = 1 + bz - a^2 z^2, \tag{14}$$

where
$$b \equiv [\{1 + \tfrac{1}{2}(\gamma - 1) M_G^2\}/(T_S/T_G)] - 1$$

and
$$a^2 \equiv \{\tfrac{1}{2}(\gamma - 1) M_G^2\}/(T_S/T_G).$$

Viscosity law. The viscosity law recommended by the original authors has been used in most cases for applying their theory to experimental conditions. When this is not possible, or no law is recommended, the following power law has been used

$$\mu \propto T^{0.76}. \tag{15}$$

Although Sutherland's viscosity law, given by

$$\frac{\mu}{\mu_G} = \frac{T}{T_G}\,\frac{T_G + 198\,^\circ\mathrm{R}}{T + 198\,^\circ\mathrm{R}} \tag{16}$$

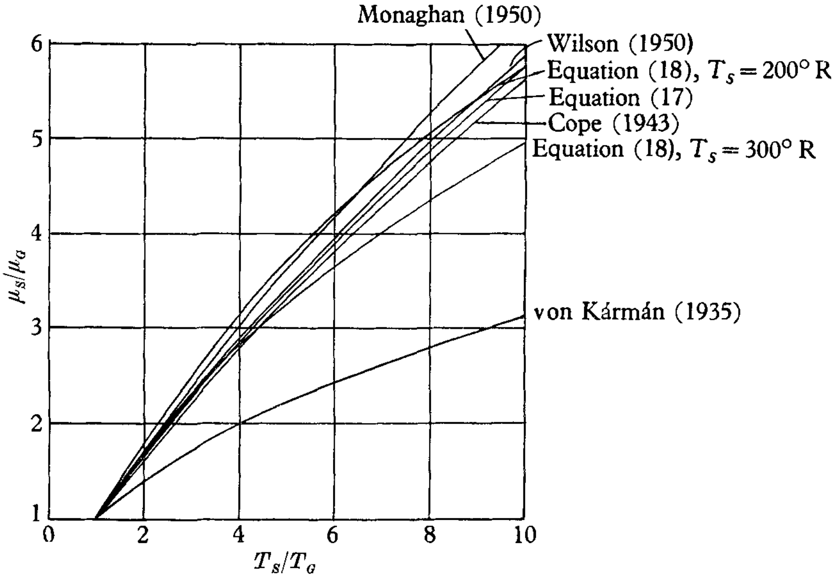

FIGURE 5. Comparison of various viscosity-temperature laws.

is more accurate than the power law, the absolute value of T_G was not reported by most experimenters. Figure 5 shows the viscosity-temperature relations used in the various theories. Since μ has only a weak influence on c_f, it is unlikely that the use of different viscosity laws for different theories has any appreciable effect on our final conclusions.

Drag laws for incompressible flow. Each of the authors whose works we have studied incorporates in his theory, implicitly or explicitly, a relationship between drag coefficient and Reynolds number (either R_δ or R_x) valid for incompressible flow. We have in each case used the relationship recommended by the author in question, without attempting to calculate separately its effect on the accuracy of the theory. However, in the Reynolds-number range of the experiments, the drag coefficients calculated from the various formulae differ only by 1 or 2 %, so there is no reason to expect that the use of a single relationship would have appreciably modified our final conclusion.

3.4. *Comparison between theories and experiments*

Twenty out of twenty-nine collected theories (see references marked with an asterisk) are compared in this report; they are believed to include all the essential assumptions used by various authors. Nine theories (theories which have been

Principal assumptions	Authors and years	R.M.S. error for adiabatic wall (%)	R.M.S. error for heat transfer (%)	Total R.M.S. error (%)
Prandtl differential equation	Smith & Harrop (1946)	29·3	37·9	32·3
	van Driest–I (1951)	13·3	17·3	14·7
	Kutateladze & Leont'ev (1961)	9·5	16·2	12·0
von Kármán differential equation	Frankl & Voishel (1937)	20·3	41·7	28·7
	Wilson (1950)	10·4	13·6	11·5
	van Driest–II (1955)	9·7	13·6	11·0
Other differential equations	Clemmow–I (1950)	11·5	21·5	15·2
	Clemmow–II (1950)	20·7	31·7	24·7
Fixed velocity profile	Cope–I (1943)	16·7	24·7	19·1
	Cope–II (1943)	12·6	25·0	17·4
	Monaghan (1950)	13·5	25·3	18·0
Reference temperature	von Kármán (1935)	25·0	38·7	29·9
	Tucker (1951)	9·6	22·5	14·9
	Young & Janssen (1952)	12·7	22·8	16·5
	Sommer & Short (1955)	12·0	17·1	13·8
	Eckert (1955)	12·2	20·2	15·1
Miscellaneous other assumptions	Donaldson (1952)	12·4	20·6	15·4
	Spence (1959)	12·2	18·2	14·3
	Winkler (1961)	14·0	23·7	17·6
	Burgraff (1962)	16·1	26·1	19·8
	Present procedure	8·6	12·5	9·9

TABLE 6. Comparison of theories with experimental data of the references marked with a cross

compared are listed in table 6) are not included, either because they still have indeterminate constants or because they involve lengthy time-consuming numerical work which is believed not to be profitable at the present state of knowledge of turbulence.

The criterion used for comparison is the root-mean-square of

$$(c_{f,\,\mathrm{exp}} - c_{f,\,\mathrm{th}})/c_{f,\,\mathrm{th}},$$

where $c_{f,\,\mathrm{exp}}$ is the experimental local or overall friction coefficient and $c_{f,\,\mathrm{th}}$ is the theoretical local or overall friction coefficient*, the corresponding experimental Reynolds number (R_δ or R_x), Mach number (M_G) and temperature ratio (T_S/T_G). In evaluating the above root-mean-square value for each of 20 theories, all the experimental data of Appendix A (plotted in figures 1–3) have been used.

The evaluation of the root-mean-square values of $(c_{f,\,\mathrm{exp}} - c_{f,\,\mathrm{th}})/c_{f,\,\mathrm{th}}$ was carried out by the Mercury digital computer of London University. A computer program was written for each of the twenty theories. Then each theory was applied to each of the 491 experimental conditions for which $c_{f,\,\mathrm{exp}}$ data were available, yielding appropriate values of $c_{f,\,\mathrm{th}}$. The root-mean-square value of $(c_{f,\,\mathrm{exp}} - c_{f,\,\mathrm{th}})/c_{f,\,\mathrm{th}}$ was then computed for each theory in an obvious manner.

The results of the comparison are shown in table 6. They give a quantitative indication of the accuracy of the various theories when compared with present empirical knowledge of the compressible turbulent boundary layer.

It is seen from table 6 that the three best theories are those of van Driest–II (1955), Wilson (1950) extended by us, and Kutateladze & Leont'ev (1961). They are all based upon the mixing-length theory used in the method of §§ 2.2 or 2.3, that is, tables 1 or 2. Table 6 also reveals that all theories exhibit a greater error when compared with the data for finite heat-transfer rates than when compared with data obtained under adiabatic conditions.

4. Development of an improved calculation procedure

4.1. *Fundamental functions*

We first seek a relation between c_f and R_δ. For the constant-pressure boundary layer, we may expect that

$$c_f = c_f(R_\delta, M_G, T_S/T_G). \tag{17}$$

The nature of the function can be determined either theoretically (§ 2) or experimentally.

Now many of the theoretical expressions, viz. theories of Clemmow–I & II (1950), Cope–II (1943), Monaghan (1950), Smith & Harrop (1946), van Driest–I & II (1951, 1955), Spence (1959), Wilson (1950), Winkler (1961) and table 5 can be written in the form

$$\tfrac{1}{2}c_f F_c = \psi_\delta(R_\delta F_{R\delta}), \tag{18}$$

where the function ψ_δ is independent of Mach number and temperature ratio, the

* For the sake of simplicity, here and on some other occasions, c_f stands for both c_f and $\bar{c}_f$, as is clear in the text.

effects of which are wholly accounted for by the functions F_c and $F_{R\delta}$. The latter functions are such that

$$\begin{aligned} F_c &= F_c(M_G, T_S/T_G), \\ &= 1, \quad \text{for} \quad M_G = 0, \quad T_S/T_G = 1; \end{aligned} \tag{19}$$

$$\begin{aligned} F_{R\delta} &= F_{R\delta}(M_G, T_S/T_G), \\ &= 1, \quad \text{for} \quad M_G = 0, \quad T_S/T_G = 1. \end{aligned} \tag{20}$$

Some of the other theoretical expressions, for example, those of Kutateladze & Leont'ev (1961), and Burgraff (1962), if expressed in the form of equation (18), would imply that $F_{R\delta}$ exhibits a weak dependence on c_f; however, this is by no means certain, as is shown by our comparison between theories and experiments (table 6) and we shall ignore this dependence.

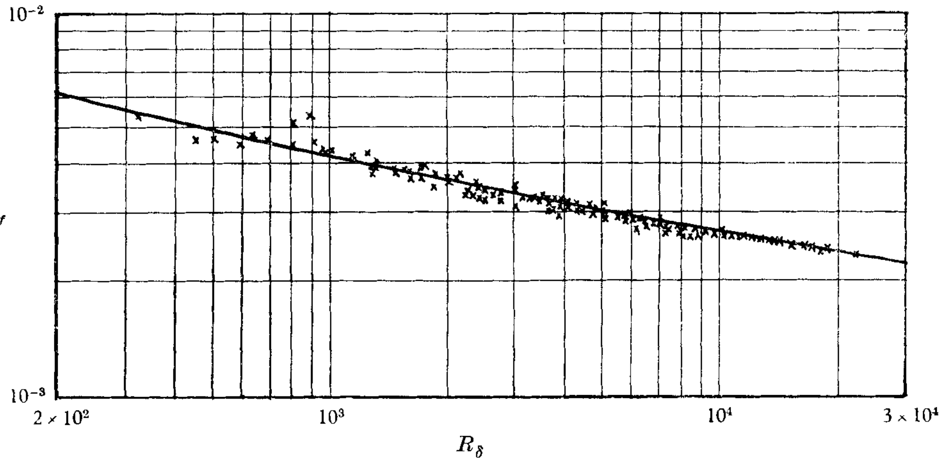

FIGURE 6. Comparison of equation (28) with uniform-property data, c_f *vs* R_δ.

Secondly, we will consider the relation between c_f and R_x. The integral momentum equation for the boundary layer on a flat plate (see Schlichting 1960, p. 536) leads to

$$\tfrac{1}{2}c_f = dR_\delta/dR_x. \tag{21}$$

Rewriting equation (21) in integral form, we obtain

$$R_x = \int_0^{R_\delta} (2/c_f)\, dR_\delta. \tag{22}$$

By multiplication of equation (22) by $F_{R\delta}/F_c$, there is obtained

$$\frac{F_{R\delta}}{F_c} R_x = \int_0^{F_{R\delta}R_\delta} \frac{2}{c_f F_c}\, d(F_{R\delta} R_\delta). \tag{23}$$

We have already postulated the existence of a unique relation between $c_f F_c$ and $R_\delta F_{R\delta}$ in equation (18), which is independent of Mach number and temperature ratio. With this, equation (23) yields

$$\tfrac{1}{2}c_f F_c = \psi_x(R_x F_{Rx}), \tag{24}$$

where the function ψ_x is independent of Mach number and temperature ratio, F_c and $F_{R\delta}$ are the same functions as those of equations (19) and (20), and F_{Rx} is related to $F_{R\delta}$ and F_c by

$$\begin{aligned} F_{Rx} &= F_{R\delta}/F_c \\ &= 1, \quad \text{for} \quad M_G = 0, \quad T_S/T_G = 1. \end{aligned} \tag{25}$$

Finally, consider $\bar{c}_f$ as a function of R_x. From the definition of $\bar{c}_f$,

$$\tfrac{1}{2}\bar{c}_f \equiv (R_x)^{-1}\int_0^{R_x} (c_f/2)\,dR_x, \tag{26}$$

it can be shown by the method of the preceding paragraph that

$$\tfrac{1}{2}\bar{c}_f F_c = \bar{\psi}(R_x F_{Rx}), \tag{27}$$

where the function $\bar{\psi}$ is again independent of Mach number and temperature ratio, and F_c and F_{Rx} are defined by equations (19) and (25).

To summarize, it has been shown that, if $F_{R\delta}$ is independent of $\frac{1}{2}c_f$, the following functions exist,

$$\tfrac{1}{2}c_f F_c = \psi_\delta(F_{R\delta}R_\delta), \tag{18}$$

$$\tfrac{1}{2}c_f F_c = \psi_x(F_{Rx}R_x), \tag{24}$$

$$\tfrac{1}{2}\bar{c}_f F_c = \bar{\psi}(F_{Rx}R_x), \tag{27}$$

where ψ_δ, ψ_x and $\bar{\psi}$ are independent of Mach number and temperature ratio. Now analytic functions exist which adequately represent the relations between $\frac{1}{2}c_f$ and R_δ, $\frac{1}{2}c_f$ and R_x, and $\frac{1}{2}\bar{c}_f$ and R_x, in uniform-density flow (Spalding 1962*a*), namely*

$$\begin{aligned} R_\delta = \tfrac{1}{6}(u_G^+)^2 + (KE)^{-1}\,[\{1-(2/Ku_G^+)\}\exp(Ku_G^+) + (2/Ku_G^+) + 1 \\ - \tfrac{1}{6}(Ku_G^+)^2 - \tfrac{1}{12}(Ku_G^+)^3 - \tfrac{1}{40}(Ku_G^+)^4 - \tfrac{1}{180}(Ku_G^+)^5], \end{aligned} \tag{28}$$

$$\begin{aligned} R_x = \tfrac{1}{12}(u_G^+)^2 + (K^3E)^{-1}\,[\{6 - Ku_G^+ + (Ku_G^+)^2\}\exp(Ku_G^+) - 6 \\ - 2Ku_G^+ - \tfrac{1}{12}(Ku_G^+)^4 - \tfrac{1}{20}(Ku_G^+)^5 - \tfrac{1}{60}(Ku_G^+)^6 - \tfrac{1}{252}(Ku_G^+)^7], \end{aligned} \tag{29}$$

$$\tfrac{1}{2}\bar{c}_f = R_\delta/R_x, \tag{30}$$

where $u_G^+ = (2/c_f)^{\frac{1}{2}}$, $K = 0{\cdot}4$ and $E = 12$.

Figures 6, 7 and 8 show the comparison between the above three functions, equations (28), (29) and (30), and the incompressible turbulent boundary-layer experimental data from those references marked with a dagger. The agreement is good throughout the whole range of Reynolds number; indeed the values of E and K have been chosen so as to give a minimum value of root-mean-square error in a manner similar to that described above, Chi (1962).† Now, our problem reduces to the determination of F_c and $F_{R\delta}$ as functions of Mach number and temperature ratio.

4.2. *Determination of the F_c-function*

Since the functions ψ_δ, ψ_x, and $\bar{\psi}$ are known [equations (28), (29) and (30)], and since numerous data for compressible turbulent boundary layers [references marked with a double dagger] have been collected, it might seem to be possible

* These are of course not the only equations which may be used; and they are certainly not the simplest. They are used because they are consistent with a formula for the universal velocity profile which is both simple and in good agreement with experimental data.

† On a c_f basis, the root-mean-square error would be about 2 %.

to deduce the F_c and $F_{R\delta}$ functions solely from experiment. An attempt to do this, however, soon showed that the data were too scanty and inaccurate to allow success. Some theoretical guidance is therefore sought for the determination of one of the functions. F_c is the obvious choice.

In § 3, it was shown that theories based upon the mixing-length hypothesis of tables 1 and 2 gave the best prediction of all the previous theories; it was also discovered that the corresponding methods lead to the following expression for F_c

$$F_c = \left[\int_0^1 (\rho/\rho_G)^{\frac{1}{2}} dz\right]^{-2}. \tag{31}$$

The expression for $F_{R\delta}$, by contrast, varies considerably from one theory to the next. Equation (31) has been adopted for the F_c function in the present theory.

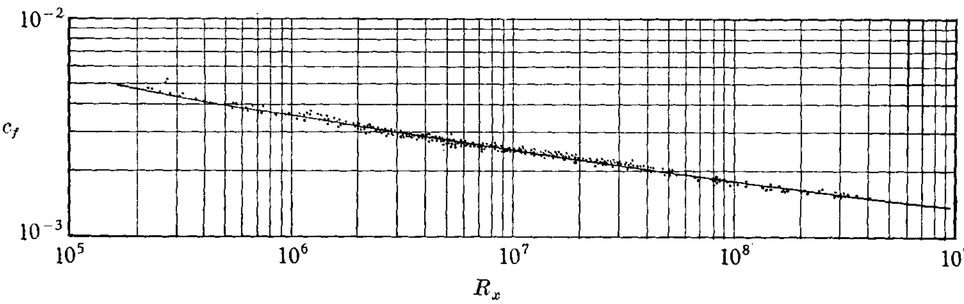

FIGURE 7. Comparison of equation (29) with uniform-property data, c_f *vs* R_x.

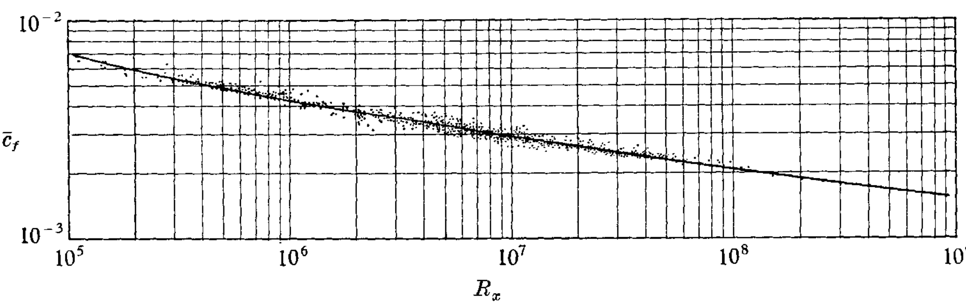

FIGURE 8. Comparison of equation (30) with uniform-property data, $\bar{c}_f$ *vs* R_x.

Evaluation of F_c from equation (31) requires the density to be expressed as a function of z, where z is defined as u/u_G. This relationship may be derived from the Reynolds analogy between energy and momentum transfer, modified for non-unity Prandtl number in the following manner.

From the Reynolds analogy, we have

$$\frac{h^0 - h^0_S}{h^0_G - h^0_S} = \frac{u - u_S}{u_G - u_S}, \tag{32}$$

where h^0 is the stagnation enthalpy, u is the velocity in the x-direction, subscripts G and S refer to the main stream and the fluid adjacent to the wall, respectively.

Now $u_S = 0$, $h^0 = c(T + \frac{1}{2}(\gamma-1)M_G^2 T_G z^2)$ for a perfect gas, $h_S^0 = h_S = cT_S$, where c is the specific heat at constant pressure, and T is the temperature in degrees absolute. Equation (32) can then be written as

$$T/T_G = (T_S/T_G) + \{1 + \tfrac{1}{2}(\gamma-1)\,M_G^2 - (T_S/T_G)\}\,z - \tfrac{1}{2}(\gamma-1)\,M_G^2 z^2. \tag{33}$$

For the adiabatic-wall case, the coefficient of z of equation (33) is zero, and T_S is equal to the adiabatic-wall temperature, $T_{ad,S}$. Hence

$$T_{ad,S}/T_G = 1 + \tfrac{1}{2}(\gamma-1)\,M_G^2. \tag{34}$$

This holds for a Prandtl number of unity. For non-unity Prandtl number,

$$T_{ad,S}/T_G = 1 + \tfrac{1}{2}r(\gamma-1)\,M_G^2, \tag{35}$$

where r is the recovery factor. For gases of $P \approx 0{\cdot}7$, measurements of recovery factor by various investigators, Brevoort & Arabian (1958), Brinich (1961), Kaye (1954), Hilton (1951), Slack (1952) and Stalder, Rubesin & Tendeland (1950), showed that the value of recovery factor lies between 0·88 and 0·9; 0·89 is a fair mean of all measurements. Now equation (33) can be modified to satisfy the boundary condition at the wall for the adiabatic-wall case, by writing

$$T/T_G = (T_S/T_G) + \{1 + \tfrac{1}{2}r(\gamma-1)\,M_G^2 - (T_S/T_G)\}\,z - \tfrac{1}{2}r(\gamma-1)\,M_G^2 z^2, \tag{36}$$

where $r = 0{\cdot}89$ for $P \approx 0{\cdot}7$. For an ideal gas at constant pressure,

$$\rho/\rho_G = (T/T_G)^{-1}. \tag{37}$$

On substitution of equation (36) into equation (37), there is obtained

$$\rho/\rho_G = [(T_S/T_G) + \{1 + \tfrac{1}{2}r(\gamma-1)\,M_G^2 - (T_S/T_G)\}\,z - \tfrac{1}{2}r(\gamma-1)\,M_G^2 z^2]^{-1}. \tag{38}$$

Hence from equations (31) and (38), we have

$$F_c = \left\{\int_0^1 \frac{dz}{[(T_S/T_G) + \{1 + \frac{1}{2}r(\gamma-1)\,M_G^2 - (T_S/T_G)\}\,z - \frac{1}{2}r(\gamma-1)\,M_G^2 z^2]^{\frac{1}{2}}}\right\}^{-2}, \tag{39}$$

where $r = 0{\cdot}89$. Equation (39) is the F_c function which we have used.

4.3. *Determination of the $F_{R\delta}$ function*

Though the theoretically derived expressions for $F_{R\delta}$ are rather uncertain, they can generally be written as

$$F_{R\delta} = (\mu_G/\mu_S)\,(\rho_S/\rho_G)^{\beta}\,(E/E_i), \tag{40}$$

where E_i is the value of E for uniform-property flow and is a constant. For example,

(*a*) In the van Driest–I method, $\beta = \frac{1}{2}$, $E = E_i$, hence

$$\begin{aligned} F_{R\delta} &= (\mu_G/\mu_S)\,(\rho_S/\rho_G)^{\frac{1}{2}} \\ &= (T_G/T_S)^{1{\cdot}26} \quad \text{for} \quad \mu_G/\mu_S = (T_G/T_S)^{0{\cdot}76}. \end{aligned} \tag{41}$$

(*b*) In the van Driest–II method, $\beta = 0$, $E = E_i$, hence

$$\begin{aligned} F_{R\delta} &= (\mu_G/\mu_S) \\ &= (T_G/T_S)^{0{\cdot}76} \quad \text{for} \quad \mu_G/\mu_S = (T_G/T_S)^{0{\cdot}76}. \end{aligned} \tag{42}$$

(*c*) In other methods, e.g. those of Kalikman (1956), Kutateladze & Leont'ev (1961)

$$E/E_i = f(T_N/T_S), \tag{43}$$

where T_N is the value of the temperature at some point near the wall.

Hence such theories commonly lead to an expression for $F_{R\delta}$ of the form

$$F_{R\delta} = (T_S/T_G)^p \, (T_N/T_S)^n, \tag{44}$$

where p and n are two constants which are still indeterminate and are to be determined from experiments as in the following paragraphs.

For the adiabatic-wall case, the temperature gradient at the wall is zero, and so the temperature near the wall is approximately equal to T_S. Hence equation (44) reduces to

$$F_{R\delta} = (T_S/T_G)^p. \tag{45}$$

Using the functions ψ_δ, ψ_x, $\overline{\psi}$ and F_c of equations (28), (29), (30) and (39), respectively, and all the collected experimental data for the adiabatic-wall case (summarized in Appendix A and figures 1–3), we have determined the value of p which gives the smallest root-mean-square value of $(c_{f,\,\mathrm{exp}} - c_{f,\,\mathrm{th}})/c_{f,\,\mathrm{th}}$. This value of p is $-0{\cdot}702$. Thus, for the adiabatic-wall case,

$$F_{R\delta} = (T_S/T_G)^{-0{\cdot}702}, \tag{46}$$

where T_S is of course the adiabatic-wall temperature which is obtained by equation (35).

The index q can be found from the drag coefficient in the presence of heat transfer. When there is heat transfer at the wall, the temperature gradient at the wall has a finite value and it is plausible that the ratio of the temperature in the vicinity of the wall to the wall temperature, T_N/T_S, is

$$T_N/T_S = 1 + z_N[d(T/T_S)/dz]_S, \tag{47}$$

where $z_N = u_N^+/u_G^+$, u_N^+ is the value of u^+ at the relevant distance from the wall. It is probable that u_N^+ is small so that u_G^+ is usually much larger than u_N^+; hence equation (47) can be written equally well as

$$T_N/T_S = \{1 + [d(T/T_S)/dz]_S\}^{z_N}. \tag{48}$$

Now, by differentiation of equation (36), we obtain

$$\left(\frac{d(T/T_S)}{dz}\right)_S = \left(1 + \tfrac{1}{2}r(\gamma-1)M_G^2 - \frac{T_S}{T_G}\right)\frac{T_G}{T_S}, \tag{49}$$

then

$$T_N/T_S \approx \left\{1 + \left[\frac{1 + \frac{1}{2}r(\gamma-1)M_G^2}{T_S/T_G} - 1\right]\right\}^{z_N}$$

$$= (T_{ad,\,S}/T_S)^{z_N}. \tag{50}$$

Substituting equation (50) into equation (44), we have

$$F_{R\delta} = (T_S/T_G)^p \, (T_{ad,\,S}/T_S)^q, \tag{51}$$

where $p = -0{\cdot}702$ obtained above and q $(= nz_N)$ is a constant to be determined empirically with the use of frictional-drag coefficient data in the presence of heat transfer. A computer program was written which varied q and minimized the root-mean-square value of $(c_{f,\,\mathrm{exp}} - c_{f,\,\mathrm{th}})/c_{f,\,\mathrm{th}}$ for all the available heat-transfer experiments, p being given the value $-0{\cdot}702$ as derived earlier. The minimum root-mean-square error was found when q was 0·772. The recommended $F_{R\delta}$ is accordingly

$$F_{R\delta} = (T_S/T_G)^{-0\cdot702}\,(T_{ad,\,S}/T_S)^{0\cdot772}, \tag{52}$$

which reduces to equation (46) for the adiabatic wall.

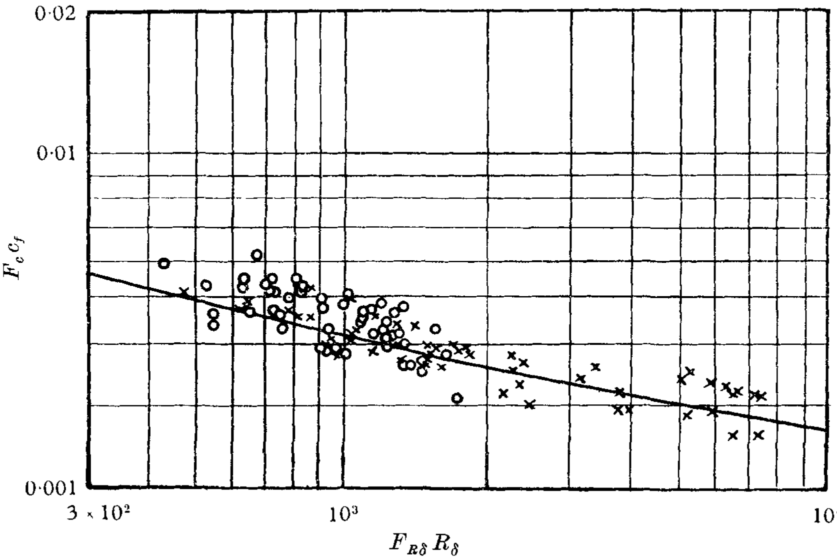

FIGURE 9. Comparison between theoretical and experimental $F_c c_f$ *vs* $F_{R\delta} R_\delta$. ×, experiments, adiabatic; ○, experiments with heat transfer; —, theory equation (28).

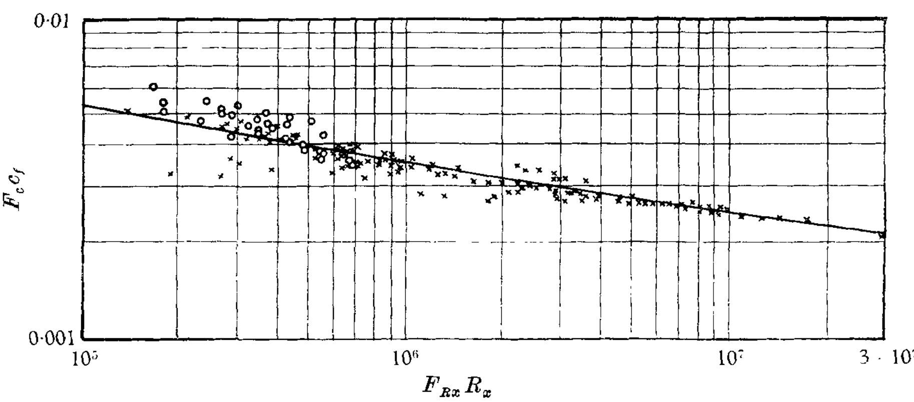

FIGURE 10. Comparison between theoretical and experimental $F_c c_f$ *vs* $F_{Rx} R_x$. ×, experiments, adiabatic; ○, experiments with heat transfer; —, theory equation (29).

4.4. *Comparison of the present method with other theories and experiments*

The root-mean-square value of $(c_{f,\,\mathrm{exp}} - c_{f,\,\mathrm{th}})\,c_{f,\,\mathrm{th}}$ for the present theory has been calculated and inserted in table 6 in order to compare it with the other theories. The present theory gives the lowest root-mean-square value, namely 9·9 %. This is to be expected because we have derived $F_{R\delta}$ directly from the experimental data. In figures 9–11, the experimental and theoretical $F_c c_f$ *vs* $F_{R\delta} R_\delta$, $F_c c_f$ *vs* $F_{Rx} R_x$ and $F_c \bar{c}_f$ *vs* $F_{Rx} R_x$ are plotted. The agreement between theory and experiments is again satisfactory.

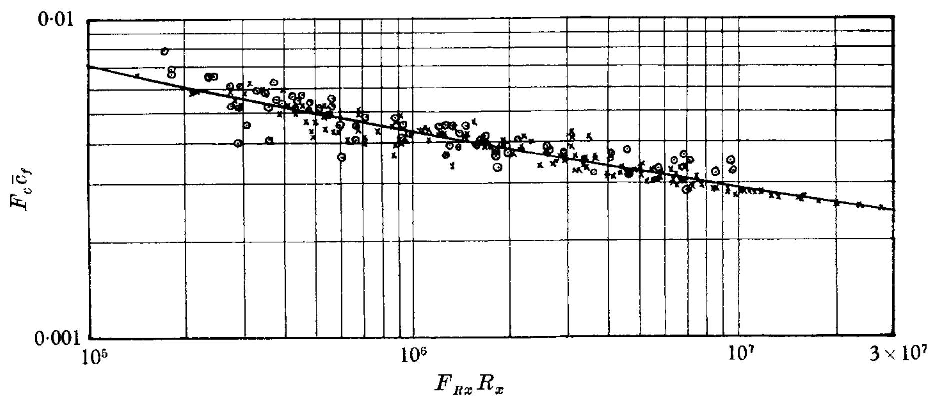

FIGURE 11. Comparison between theoretical and experimental $F_c \bar{c}_f$ *vs* $F_{Rx} R_x$. ×, experiments, adiabatic; ○, experiments with heat transfer; —, theory equation (30).

$F_c c_f$	$F_c \bar{c}_f$	$F_{R\delta} R_\delta$	$F_{Rx} R_x$	$F_c c_f$	$F_c \bar{c}_f$	$F_{R\delta} R_\delta$	$F_{Rx} R_x$
0·0010	0·001117	$2{\cdot}878 \times 10^7$	$5{\cdot}758 \times 10^{10}$	0·0060	0·008205	233·0	$5{\cdot}679 \times 10^4$
0·0015	0·001716	$3{\cdot}955 \times 10^5$	$4{\cdot}610 \times 10^8$	0·0065	0·009105	177·6	$3{\cdot}901 \times 10^4$
0·0020	0·002333	$5{\cdot}425 \times 10^4$	$4{\cdot}651 \times 10^7$	0·0070	0·010042	140·4	$2{\cdot}796 \times 10^4$
0·0025	0·002967	$1{\cdot}386 \times 10^4$	$9{\cdot}340 \times 10^6$	0·0075	0·011014	114·4	$2{\cdot}078 \times 10^4$
0·0030	0·003621	5030	$2{\cdot}778 \times 10^6$	0·0080	0·012016	95·62	$1{\cdot}592 \times 10^4$
0·0035	0·004299	2283	$1{\cdot}062 \times 10^6$	0·0085	0·01304	92·49	$1{\cdot}251 \times 10^4$
0·0040	0·005006	1208	$4{\cdot}828 \times 10^5$	0·0090	0·01409	70·91	$1{\cdot}006 \times 10^4$
0·0045	0·005747	716·0	$2{\cdot}492 \times 10^5$	0·0095	0·01516	62·55	$8{\cdot}253 \times 10^3$
0·0050	0·006526	462·3	$1{\cdot}417 \times 10^5$	0·0100	0·01624	55·87	$6{\cdot}883 \times 10^3$
0·0055	0·007345	319·4	$8{\cdot}697 \times 10^4$	0·0105	0·01732	50·46	$5{\cdot}826 \times 10^3$

TABLE 7. Values of $F_c c_f$, $F_c \bar{c}_f$, $F_{R\delta} R_\delta$ and $F_{Rx} R_x$

4.5. *Summary of results*

To facilitate calculation, the main results derived earlier in this section are presented in the form of tables and figures. Table 7 gives the corresponding values of $F_c c_f$ and $F_c \bar{c}_f$ *vs* $F_{R\delta} R_\delta$ and $F_{Rx} R_x$, table 8 gives the values of F_c at various M_G and T_S/T_G, and table 9 gives the values of $F_{R\delta}$ at various M_G and T_S/T_G. Values from tables 8 and 9 are plotted in figure 12 for convenience of use.

4.6. *Recommended method of calculation*

In the most common cases, the problem is to find the drag coefficient when the Reynolds number, Mach number and temperature ratio are known. The procedure for solving this problem by use of the present method is as follows. First, the value of F_c is determined from table 8 or figure 12. Then the value of $F_{R\delta}$ is

T_S/T_G \ M_G	0	1	2	3	4	5	6	7
0·05	0·3743	0·4036	0·4884	0·6222	0·7999	1·0184	1·2759	1·5713
0·1	0·4331	0·4625	0·5477	0·6829	0·8628	1·0842	1·3451	1·6444
0·2	0·5236	0·5530	0·6388	0·7756	0·9584	1·1836	1·4491	1·7534
0·3	0·5989	0·6283	0·7145	0·8523	1·0370	1·2649	1·5337	1·8418
0·4	0·6662	0·6957	0·7821	0·9208	1·1069	1·3370	1·6083	1·9194
0·5	0·7286	0·7580	0·8446	0·9839	1·1713	1·4031	1·6767	1·9903
0·6	0·7873	0·8168	0·9036	1·0434	1·2318	1·4651	1·7405	2·0564
0·8	0·8972	0·9267	1·0137	1·1544	1·3445	1·5802	1·8589	2·1785
1	1·0000	1·0295	1·1167	1·2581	1·4494	1·6871	1·9684	2·2913
2	1·4571	1·4867	1·5744	1·7176	1·9130	2·1572	2·4472	2·7809
3	1·8660	1·8956	1·9836	2·1278	2·3254	2·5733	2·8687	3·2092
4	2·2500	2·2796	2·3678	2·5126	2·7117	2·9621	3·2611	3·6066
5	2·6180	2·6477	2·7359	2·8812	3·0813	3·3336	3·6355	3·9847
6	2·9747	3·0044	3·0927	3·2384	3·4393	3·6930	3·9971	4·3493
8	3·6642	3·6938	3·7823	3·9284	4·1305	4·3863	4·6937	5·0505
10	4·3311	4·3608	4·4493	4·5958	4·7986	5·0559	5·3657	5·7259
12	4·9821	5·0117	5·1003	5·2470	5·4504	5·7088	6·0204	6·3832
14	5·6208	5·6505	5·7391	5·8860	6·0898	6·3491	6·6621	7·0271
16	6·2500	6·2797	6·3683	6·5153	6·7196	6·9795	7·2937	7·6603
18	6·8713	6·9010	6·9897	7·1368	7·3413	7·6019	7·9170	8·2851
20	7·4861	7·5157	7·6045	7·7517	7·9564	8·2175	8·5334	8·9027
25	9·0000	9·0297	9·1184	9·2658	9·4711	9·7330	10·0505	10·4222
30	10·4886	10·5183	10·6071	10·7546	10·9602	11·2228	11·5415	11·9149

T_S/T_G \ M_G	8	9	10	11	12	13	14	15
0·05	1·9041	2·3738	2·6803	3·1233	3·6027	4·1186	4·6707	5·2591
0·1	1·9812	2·3552	2·7660	3·2134	3·6976	4·2180	4·7748	5·3680
0·2	2·0958	2·4756	2·8925	3·3462	3·8366	4·3636	4·9269	5·5267
0·3	2·1882	2·5723	2·9937	3·4522	3·9974	4·4792	5·0475	5·6523
0·4	2·2692	2·6569	3·0820	3·5443	4·0435	4·5794	5·1518	5·7608
0·5	2·3429	2·7336	3·1620	3·6276	4·1303	4·6697	5·2458	5·8584
0·6	2·4115	2·8049	3·2362	3·7048	4·2105	4·7531	5·3324	5·9483
0·8	2·5379	2·9360	3·3721	3·8459	4·3570	4·9051	5·4901	6·1117
1	2·6542	3·0562	3·4966	3·9748	4·4905	5·0434	5·6333	6·2599
2	3·1564	3·5725	4·0282	4·5228	5·0556	5·6263	6·2345	6·8801
3	3·5929	4·0184	4·4846	4·9904	5·5353	6·1187	6·7401	7·3993
4	3·9964	4·4290	4·9030	5·4176	5·9719	6·5653	7·1972	7·8673
5	4·3792	4·8174	5·2979	5·8196	6·3817	6·9833	7·6240	8·3033
6	4·7477	5·1905	5·6764	6·2041	6·7727	7·3814	8·0297	8·7169
8	5·4549	5·9050	6·3994	6·9368	7·5161	8·1365	8·7972	9·4977
10	6·1347	6·5904	7·0913	7·6363	8·2241	8·8539	9·5247	10·2359
12	6·7955	7·2556	7·7618	8·3129	8·9077	9·5452	10·2245	10·9449
14	7·4422	7·9058	8·4164	8·9727	9·5734	10·2174	10·9040	11·6321
16	8·0778	8·5444	9·0587	9·6194	10·2251	10·6748	11·5676	12·3026
18	8·7045	9·1737	9·6912	10·2556	10·8657	11·5204	12·2187	12·9598
20	9·3238	9·7952	10·3154	10·8832	11·4971	12·1562	12·8595	13·6059
25	10·8467	11·3225	11·8482	12·4227	13·0446	13·7128	14·4263	15·1841
30	12·3418	12·8209	13·3509	13·9305	14·5586	15·2339	15·9556	16·7225

TABLE 8. Values of F_c at various M_G and T_S/T_G

T_S/T_G \ M_G	0	1	2	3	4	5	6	7
0·05	82·7405	93·8950	125·3092	173·1153	234·1638	306·3489	388·2642	478·9229
0·1	29·7852	33·8006	45·1092	62·3185	84·2949	110·2803	139·7684	172·4040
0·2	10·7221	12·1676	16·2385	22·4336	30·3447	39·6990	50·3142	62·0625
0·3	5·8983	6·6934	8·9328	12·3407	16·6926	21·8384	27·6779	34·1406
0·4	3·8598	4·3801	5·8456	8·0757	10·9236	14·2910	18·1123	22·3414
0·5	2·7779	3·1524	4·2071	5·8121	7·8618	10·2853	13·0355	16·0792
0·6	2·1233	2·4095	3·2157	4·4424	6·0091	7·8615	9·9636	12·2900
0·8	1·3895	1·5768	2·1043	2·9071	3·9323	5·1445	6·5201	8·0425
1	1·0000	1·1348	1·5145	2·0923	2·8301	3·7025	4·6926	5·7883
2	0·3600	0·4085	0·5452	0·7532	1·0188	1·3328	1·6892	2·0837
3	0·1980	0·2247	0·2999	0·4143	0·5604	0·7332	0·9292	1·1462
4	0·1296	0·1471	0·1963	0·2711	0·3667	0·4798	0·6081	0·7501
5	0·0933	0·1058	0·1412	0·1951	0·2639	0·3453	0·4377	0·5398
6	0·0713	0·0809	0·1080	0·1491	0·2017	0·2639	0·3345	0·4126
8	0·0466	0·0529	0·0706	0·0976	0·1320	0·1727	0·2189	0·2700
10	0·0336	0·0381	0·0508	0·0702	0·0950	0·1243	0·1575	0·1943
12	0·0257	0·0291	0·0389	0·0537	0·0726	0·0950	0·1204	0·1485
14	0·0204	0·0232	0·0310	0·0428	0·0579	0·0757	0·0959	0·1183
16	0·0168	0·0191	0·0254	0·0351	0·0475	0·0622	0·0788	0·0972
18	0·0141	0·0160	0·0214	0·0295	0·0400	0·0523	0·0662	0·0817
20	0·0121	0·0137	0·0183	0·0253	0·0342	0·0447	0·0567	0·0700
25	0·0087	0·0099	0·0132	0·0182	0·0246	0·0322	0·0408	0·0503
30	0·0066	0·0075	0·0101	0·0139	0·0188	0·0246	0·0312	0·0385

T_S/T_G \ M_G	8	9	10	11	12	13	14	15
0·05	577·5949	683·7162	796·8344	916·5768	1042·629	1174·722	1312·620	1456·116
0·1	207·9243	246·1261	286·8467	329·9519	375·3286	422·8798	472·5207	524·1767
0·2	74·8492	88·6012	103·2599	118·7770	135·1119	152·2295	170·0993	188·6946
0·3	41·1745	48·7395	56·8032	65·3392	74·3250	83·7414	93·5716	103·8009
0·4	26·9444	31·8949	37·1718	42·7577	48·6380	54·8000	61·2328	67·9268
0·5	19·3920	22·9549	26·7527	30·7729	35·0050	39·4398	44·0696	48·8873
0·6	14·8221	17·5454	20·4482	23·5210	26·7557	30·1455	33·6842	37·3665
0·8	9·6995	11·4816	13·3812	15·3920	17·5088	19·7271	22·0428	24·4525
1	6·9808	8·2634	9·6305	11·0777	12·6012	14·1977	15·8643	17·5986
2	2·5130	2·9747	3·4668	3·9878	4·5362	5·1109	5·7109	6·3352
3	1·3824	1·6364	1·9071	2·1937	2·4954	2·8115	3·1416	3·4850
4	0·9046	1·0708	1·2480	1·4355	1·6330	1·8398	2·0558	2·2806
5	0·6511	0·7707	0·8982	1·0332	1·1752	1·3241	1·4796	1·6413
6	0·4976	0·5891	0·6862	0·7897	0·8983	1·0121	1·1309	1·2545
8	0·3256	0·3855	0·4493	0·5168	0·5878	0·6623	0·7401	0·8210
10	0·2344	0·2774	0·3233	0·3719	0·4231	0·4767	0·5326	0·5909
12	0·1791	0·2121	0·2471	0·2843	0·3234	0·3643	0·4071	0·4516
14	0·1427	0·1690	0·1969	0·2265	0·2576	0·2903	0·3244	0·3598
16	0·1172	0·1388	0·1617	0·1860	0·2116	0·2384	0·2664	0·2955
18	0·0985	0·1167	0·1359	0·1564	0·1779	0·2004	0·2239	0·2484
20	0·0844	0·0999	0·1164	0·1339	0·1523	0·1716	0·1917	0·2127
25	0·0607	0·0719	0·0838	0·0964	0·1096	0·1235	0·1380	0·1531
30	0·0464	0·0549	0·0640	0·0737	0·0838	0·0944	0·1055	0·1170

TABLE 9. Values of $F_{R\delta}$ at various M_G and T_S/T_G

determined from equation (52), table 9 or figure 12, and where necessary the value of F_{Rx} is obtained from the equation

$$F_{Rx} = F_{R\delta}/F_c. \tag{25}$$

Finally, by using the input value of R_δ (or R_x) and the values of $F_{R\delta}$ (or F_{Rx}) and F_c above, c_f or $\bar{c}_f$ can be obtained from table 7 or figures 9–11.

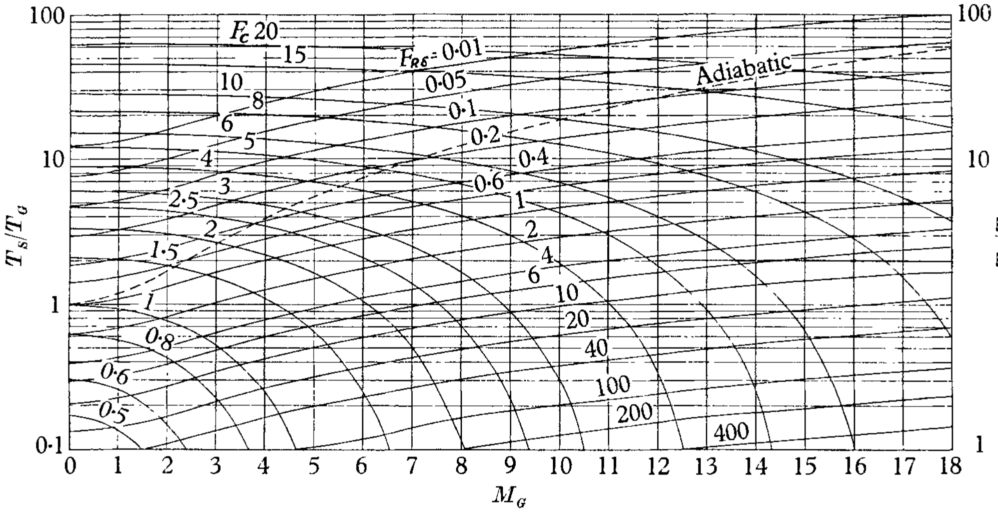

FIGURE 12. Chart of constant F_c and $F_{R\delta}$ lines in T_S/T_G and M_G co-ordinates.

The above calculation can be performed in a few minutes with an accuracy of 1 %. The latter is of course well within the limit of experimental accuracy at present.

5. Conclusions

In conclusion, the results of this work can be summarized as follows.

A procedure has been developed semi-empirically for predicting the drag coefficient on a smooth surface of zero stream-wise pressure gradient at various Reynolds numbers, Mach numbers and ratios of surface temperature to stream temperature.

The extent to which the procedure correlates the existing experimental data can be judged by inspection of figures 9–11, whereby it must be remembered that the experiments have been carried out in several entirely different pieces of apparatus and are not of high or uniform accuracy. The correlation is better than that given by any of the other existing theories as can be seen from table 6. The value of the present procedure is that it does not make use of the more arbitrary assumptions of earlier theories; it lets the data speak for themselves.

The procedure is simple and quick to use in engineering calculations and its accuracy is only limited (at the present time) by the accuracy of experimental data from which it is in part derived.

The necessary auxiliary functions have been tabulated (tables 7–9) and plotted in figures 9–12 for ready reference. However, it must be remembered that experiments have not yet been carried out over the whole range of conditions covered by the tables and figures. Figure 4 shows how remarkably restricted has been the range of experimental conditions so far.

The procedure is capable of greater refinement when more accurate experimental data are available, say by modification of the $F_{R\delta}$ function. It can also be extended to include mass transfer (Spalding 1962*b*).

Finally, it should be noted that the calculation procedure which has been recommended is based on no new physical hypothesis. The expression recommended for F_c implies the assumption of one or other variety of the mixing-length theory; but the expression for $F_{R\delta}$ is entirely empirical. It may indeed be rather hard to find a physical hypothesis to fit the empirically derived $F_{R\delta}$ function; for, whereas the exponent of (T_S/T_G) in equation (52) has a sign and magnitude which allows us to ascribe its effects to the role of the viscosity near the wall, the sign of the exponent of $(T_{ad,S}/T_S)$ is quite unexpected. This point certainly deserves explanation. However, we have thought it better at the present stage to provide quantitative results against which old and new hypotheses can be tested than to advance such hypotheses ourselves.

REFERENCES

†ABBOT, I. H. 1953 *AGARD* Memo. AG/8M4.

BREVOORT, M. J. & ARABIAN, B. D. 1958 *Nat. Adv. Comm. Aero., Wash., Tech. Note*, no. 4248.

BRINICH, P. F. 1961 *Nat. Aero. Space Admin., Tech. Note*, no. D-1047.

†BRINICH, P. F. & DIACONIS, N. S. 1952 *Nat. Adv. Comm. Aero., Wash., Tech. Note*, no. 2742.

*BURGRAFF, O. R. 1962 *J. Aero. Sci.* **29**, 434.

CHAPMAN, D. R. & KESTER, R. H. 1953 *J. Aero. Sci.* **20**, 441.

†CHAPMAN, D. R. & KESTER, R. M. 1954 *Nat. Adv. Comm. Aero., Wash., Tech. Note*, no. 3097.

CHI, S. W. 1962 Unpublished work at Imperial College.

*CLEMMOW, D. M. 1950 *Aero. Res. Counc., London*, no. 14051, F.M. 1568, DGWRD Rep. 50/6.

†COLES, D. 1954 *J. Aero. Sci.* **21**, 433.

*COLES, D. E. 1962 *Rand Corporation*, Rep. no. R-403-PR.

*COPE, W. F. 1943 *Aero. Res. Counc., London, Rep. & Mem.*, no. 2840.

†COPE, W. F. 1952 *Proc. Roy. Soc.* A, **215**, 84.

†‡DAHWAN, S. 1952 *Nat. Adv. Comm. Aero., Wash., Tech. Note*, no. 2567.

*DEISSLER, R. G. & LOEFFLER, A. L. 1959 *Nat. Aero. Space Admin., Tech. Rep.*, no. R-17.

*DONALDSON, C. dup 1952 *Nat. Adv. Comm. Aero., Wash., Tech. Note*, no. 2962.

*DORRANCE, W. H. 1960 *Convair Sci. Res. Lab. Res. Rep.* no. 6.

‡DUTTON, R. A. 1957 *Aero. Res. Counc., London, Rep. & Mem.*, no. 3058.

*ECKERT, E. R. G. 1955 *J. Aero. Sci.* **22**, 585.

‡FALKNER, V. M. 1943 *Aircraft Engng*, **15**, 65.

*FERRARI, C. 1950 *Quart. Appl. Math.* **18**, 33.

*FRANKL, F. & VOISHEL, V. 1937 Translation *Nat. Adv. Comm. Aero., Wash., Tech. Note*, no. 1052 (1943).

†GODDARD, F. E. 1959 *J. Aero./Sp. Sci.* **26**, 1.

†HAKKINEN, R. J. 1955 *Nat. Adv. Comm. Aero., Wash., Tech. Note*, no. 3486.

‡HAMA, F. R. 1947 *Rep. Inst. Sci. and Tech., Tokyo, Japan*, **1**, 13 and 19.

†Hill, F. K. 1956 *J. Aero. Sci.* **23**, 35.
†Hill, F. K. 1959 *Phys. Fluids*, **2**, 668.
Hilton, W. F. 1951 *J. Aero. Sci.* **18**, 97.
‡Hughes, G. 1952 *Trans. Inst. Nav. Arch.* **94**, 287.
*Kalikman, L. E. 1959 *Dokl. Akad. Nauk, SSSR*, **106**, 123.
Kaye, J. 1954 *J. Aero. Sci.* **21**, 117.
‡Kempf, G. 1929 *Werft, Reed., Hafen.* **11**, 234.
‡Klebanoff, P. S. & Diehl, Z. W. 1951 *Nat. Adv. Comm. Aero., Wash., Tech. Note*, no. 2475.
†Korkegi, R. H. 1956 *J. Aero. Sci.* **23**, 97.
*Kosterin, S. I. & Koshmarov, Y. A. 1960 *Soviet Phys.* **4**, 819.
*Kutateladze, S. S. & Leont'ev, A. I. 1961 *Discussion of Heat and Mass Transfer, Akad. Nauk BSSR, Minsk*, 1, Translation TIL T5258.
‡Landweber, L. & Siao, T. T. 1958 *J. Ship Res.* **1**, 21.
*Li, T. Y. & Nagamatsu, H. T. 1951 *J. Aero. Sci.* **18**, 696.
*Lin, C. C. & Shen, S. F. 1951 *Nat. Adv. Comm. Aero., Wash., Tech. Note*, no. 2542.
‡Ludwig, H. & Tillmann, W. 1949 Translation *Nat. Adv. Comm. Aero., Wash., Tech. Mem.*, no. 1285.
†‡Matting, F. M., Chapman, D. R., Nyholm, J. R. & Thomas, A. G. 1951 *Nat. Aero. Space Admin., Tech. Rep.*, no. R-82.
‡Mickley, H. S. & Davis, R. S. 1957 *Nat. Adv. Comm. Aero., Wash., Tech. Note*, no. 4017.
*Monaghan, R. J. 1950 *Aero. Res. Counc., London*, no. CP 45.
†Monaghan, R. J. & Cooke, J. R. 1953*a* *Aero. Res. Counc., London*, no. CP 139.
†Monaghan, R. J. & Cooke, J. R. 1953*b* *Aero. Res. Counc., London*, no. CP 140.
†Monaghan, R. J. & Johnson, J. E. 1952 *Aero. Res. Counc., London*, no. CP 64.
†O'Donell, R. M. 1954 *Nat. Adv. Comm. Aero., Wash., Tech. Note*, no. 3122.
†Pappas, C. C. 1954 *Nat. Adv. Comm. Aero., Wash., Tech. Note*, no. 3222.
Peterson, J. B. 1963 *Nat. Aero. Space Admin., Tech. Note*, no. D-1795.
*†Rubesin, M. W., Maydew, R. C. & Varga, S. A. 1951 *Nat. Adv. Comm. Aero., Wash., Tech. Note*, no. 2305.
Schlichting, H. 1960 *Boundary Layer Theory*, 2nd ed. Translated by J. Kestin. London: McGraw-Hill.
‡Schoenherr, K. E. 1932 *Trans. Soc. Nav. Arch. Mar. Engrs*, **40**, 279.
‡Schultz-Grunow, F. 1940 Translation *Nat. Adv. Comm. Aero., Wash., Tech. Note*, no. 986.
*Shen, S. F. 1951 *Nat. Adv. Comm. Aero., Wash., Tech. Note*, no. 2543.
Slack, E. G. 1952 *Nat. Adv. Comm. Aero., Wash., Tech. Note*, no. 2686.
‡Smith, D. W. & Walker, J. H. 1958 *Nat. Adv. Comm. Aero., Wash., Tech. Note*, no. 423.
*Smith, F. & Harrop, R. 1946 *Roy. Aircraft Estmt, Tech. Note*, Aero. 1759.
*†Sommer, S. C. & Short, B. J. 1955 *Nat. Adv. Comm. Aero., Wash., Tech. Note*, no. 3391.
Spalding, D. B. 1962*a* *Int. J. Heat Mass Transfer*, **5**, 1133.
Spalding, D. B. 1962*b* *Northern Research and Engineering Corporation, Camb., Mass. Rep.* no. 1058-1.
*Spence, D. A. 1959 *Roy. Aircraft Estmt, Rep.* Aero. 2631.
†Spivak, H. M. 1950 *Aero. Phys. Lab., Nor. Am. Aviation, Inc., Rep.* no. CM-615, CAL-1052.
Stalder, J. R., Rubesin, M. W. & Tendeland, T. 1950 *Nat. Adv. Comm. Aero., Wash., Tech. Note*, no. 2077.
*Tucker, M. 1951 *Nat. Adv. Comm. Aero., Wash., Tech. Note*, no. 2337.

*van Driest, E. R. 1951 *J. Aero. Sci.* **18**, 145.
*van Driest, E. R. 1955 *50 Years of Boundary Layer Theory* (Ed. H. Görtler and W. Tollmien), p. 257. Braunschweig: F. Vieweg u. Sohn.
*von Kármán, Th. 1935 *Proc. 5th Volta Congress, Rome*, p. 255.
‡Wieghardt, K. 1944 Translation *Nat. Adv. Comm. Aero., Wash., Tech. Mem.*, no. 1314 (1951).
*†Wilson, R. E. 1950 *J. Aero. Sci.* **17**, 585.
*†Winkler, E. M. 1961 *J. Appl. Mech., Trans A.S.M.E.* **28**, Ser. E, 323.
*Young, C. B. M. & Janssen, E. 1952 *J. Aero. Sci.* **19**, 229.

Appendix

Summary of the methods of evaluating R_δ integral, approximations A and B, appearing in tables 1–4

Approximate analytical (A)

Taking equation (3) of § 2.2, for example, we have

$$R_\delta = \frac{\mu_S K u_G^{+2}}{\mu_G E} \int_0^1 \phi^3 z(1-z) \exp\left\{K u_G^+ \int_0^z \phi\, dz\right\} dz. \tag{3}$$

As the magnitude of the integrand is small at small z,

$$\int_0^z \phi\, dz$$

is replaced by Nz, where

$$N = \frac{1}{0{\cdot}9} \int_0^{0\cdot 9} \phi\, dz;$$

the equation (3) now becomes

$$R_\delta = \frac{\mu_S K u_G^{+2}}{\mu_G E} \int_0^1 \phi^3 z(1-z) \exp\,(KNu_G^+ z)\, dz. \tag{A 1}$$

On integrating equation (A 1) by parts twice, there is obtained

$$\begin{aligned} R_\delta &= \frac{\mu_S u_G^+}{\mu_G EN} \Big[\phi^3 z(1-z) \exp\,(KNu_G^+ z) \\ &\qquad - \int_0^1 [\phi^3(1-2z) + z(1-z)\,(d\phi^3/dz)] \exp\,(KNu_G^+ z)\, dz\Big]_0^1 \\ &= \frac{\mu_S}{\mu_G KN^2 E}\Big[\phi^3 \exp\,(KNu_G^+ z)\Big]_0^1 + \text{smaller terms} \\ &\approx \frac{\mu_S \phi_G^3}{\mu_G KEN^2} \exp\,(KNu_G^+ z). \end{aligned} \tag{A 2}$$

Hence

$$R_\delta = \frac{\mu_S \phi_G^3}{\mu_G N^2 KE} \exp\left\{KN\left(\frac{2T_G}{c_f T_S}\right)^{\frac{1}{2}}\right\}. \tag{A 3}$$

Approximate analytical (B)

Taking equation (3) of § 2.2, for example, we have

$$R_\delta = \frac{\mu_S K u_G^{+2}}{\mu_G E} \int_0^1 \phi^3 z(1-z) \exp\left(K u_G^+ \int_0^z \phi\, dz\right) dz. \tag{3}$$

Equation (3) is re-written as

$$R_\delta = \frac{\mu_S K u_G^{+2}}{\mu_G E} \exp\left(K u_G^+ \int_0^1 \phi \, dz\right) \int_0^1 \phi^3 z(1-z) \exp\left(K u_G^+ \int_1^z \phi \, dz\right) dz. \quad \text{(B 1)}$$

Replace $\exp\left(K u_G^+ \int_1^z \phi \, dz\right)$ by z^n,

where n is so chosen that the gradient is the same, then, on differentiation, we have $K u_G^+ \phi = n$. Now equation (B 1) can be re-written as

$$\begin{aligned} R_\delta &\approx \frac{\mu_S K u_G^{+2}}{\mu_G E} \exp\left(K u_G^+ \int_0^1 \phi \, dz\right) \int_0^1 \phi^3 z(1-z) z^n \, dz \\ &\approx \frac{\mu_S \phi_G^3 K u_G^{+2}}{\mu_G E} \exp\left(K u_G^+ \int_0^1 \phi \, dz\right) \int_0^1 (z^{n+1} - z^{n+2}) \, dz \\ &= \frac{\mu_S \phi_G^3 K u_G^+ \exp\left(K u_G^+ \int_0^1 \phi \, dz\right)}{\mu_G [E(K\phi_G u_G^+ + 2)(K\phi u_G^+ + 3)]}. \end{aligned} \quad \text{(B 2)}$$

As $K u_G^+ \phi \gg 3$ in general, equation (B 2) can be approximately written as

$$R_\delta = \frac{\mu_S \phi_G}{\mu_G K E} \exp\left(K u_G^+ \int_0^1 \phi \, dz\right). \quad \text{(B 3)}$$

Hence

$$R_\delta = \frac{\mu_S \phi_G}{\mu_G K E} \exp\left\{K \left(\int_0^1 \phi \, dz\right) \left(\frac{2T_G}{c_f T_S}\right)^{\frac{1}{2}}\right\}. \quad \text{(B 4)}$$